Limited Topological Alteration of the T7 RNA Polymerase Active Center at Intrinsic Termination Sites†

Marc Boudvillain,* Annie Schwartz, and A. Rachid Rahmouni

Centre de Biophysique Moléculaire, CNRS, rue Charles Sadron, 45071 Orléans cedex 2, France

Received June 27, 2001; Revised Manuscript Received November 27, 2001

ABSTRACT: Transcription terminators trigger the dissociation of RNA polymerase elongation complexes and the release of RNA products at specific DNA template positions. The mechanism by which these signals alter the catalytic properties of the highly processive elongation transcription complexes is unclear. Here, we propose that intrinsic terminators impede transcript elongation by promoting a misarrangement of reactants and catalytic effectors within the active site of T7 RNA polymerase. In effect, a productive catalytic coordination network can be readily restored when Mg^{2+} effectors are replaced by the more "relaxing" Mn^{2+} ions, leading to transcript elongation beyond the termination point. This Mn^{2+}-dependent incorporation of additional nucleotides occurs within unstable transcription complexes that ultimately dissociate at positions downstream from the normal termination site. Thus, Mn^{2+} coordination in the polymerase active center can compensate for the disruptive but limited perturbation of the catalytic arrangement of reactants that accompany larger structural changes of the transcription complex triggered by termination signals. These results provide evidence that the geometry of the catalytic coordination network within the active site is a crucial component of RNA polymerase catalysis. Limited variations of the active site architecture are sufficient to confer tight control of the RNA polymerase function and, thus, may ubiquitously benefit signals regulating transcription.

Transcription, the crucial initial step of gene expression, is regulated by complex intrinsic and factor-dependent signals. During the processive phase of transcript elongation, three major classes of signals (pausing, arrest, and termination) interfere with the RNA synthesis (*1*, *2*). The pause and arrest signals induce transient and irreversible blocks, respectively, to transcript elongation within stable ternary transcription complexes, whereas the termination signals trigger the dissociation of the complexes and the release of the RNA products. Despite their different outcomes, the three kinds of signals share the ability to preclude phosphoryl transfer reactions within the RNA polymerase (RNAP)[1] active site. However, the mechanistic principles underlying this inactivation process remain largely uncharacterized.

Much biochemical and structural data suggest that the RNAP-dependent addition of nucleotides to the growing RNA chain rests on a simple two-metal ion mechanism (*3*−*5*). An important implication of this mechanism is that the RNAP amino acids do not directly participate in the chemical reaction. Rather, active site residues orchestrate the proper orientation of reactants and metal ions so that the latter can effect the activation of the attacking 3′-OH and the stabilization of the developing negative charges during the in-line SN_2 phosphoryl transfer reaction (Figure 1A). From this mechanism, two different ways of inactivating nucleotide addition can be envisioned. The reactants (the RNA 3′-OH and the incoming rNTP) or the metal effectors (two Mg^{2+} ions) may be misaligned within the active site so that the catalytic coordination network (Figure 1A) is disrupted. Inactivation would then result from local architectural distortions. As transition-state stabilization should rely heavily on active site geometry, this mechanism could provide a versatile means of regulating the RNAP activity at a low energetic cost. There are already indications that transcription complexes utilize such a strategy to discriminate between correct and incorrect nucleotides (*6*−*8*). Alternatively, reactants may be completely extruded from the active site (or prevented from entering it), leaving it partially or totally empty. Current models for pause, arrest, and termination signals which feature alterations of the lateral stability of the transcription complex (such as backward sliding) (*1*, *9*) favor this latter mechanism.

Transcript elongation by the bacteriophage T7 and SP6 RNAPs can be terminated by two distinct classes of intrinsic termination signals (*10*, *11*). Class I signals are reminiscent of the bacterial Rho-independent termination signals, of which some are genuine terminators for the bacteriophage enzymes (*12*−*14*). Class I terminators are characterized by a DNA template sequence of dyad symmetry followed by an A-rich motif that leads to the formation of an RNA transcript containing a hairpin structure upstream from a U-rich run of six to eight nucleotides. It is thought that hairpin-dependent termination signals mediate formation of an intermediate state of the ternary transcription complex in which transcript elongation is impeded (*9*, *15*−*17*). Destabilization of the intermediate complex could result from the

† This research was supported in part by the Association pour la Recherche sur le Cancer (Grant 5560) and by the Ligue contre le Cancer (comité du Loiret).

* To whom correspondence should be addressed. Phone: +33 238 25 55 51. Fax: +33 238 63 15 17. E-mail: boudvill@cnrs-orleans.fr.

[1] Abbreviation: RNAP, RNA polymerase.

10.1021/bi011358q CCC: $22.00
Published on Web 02/06/2002

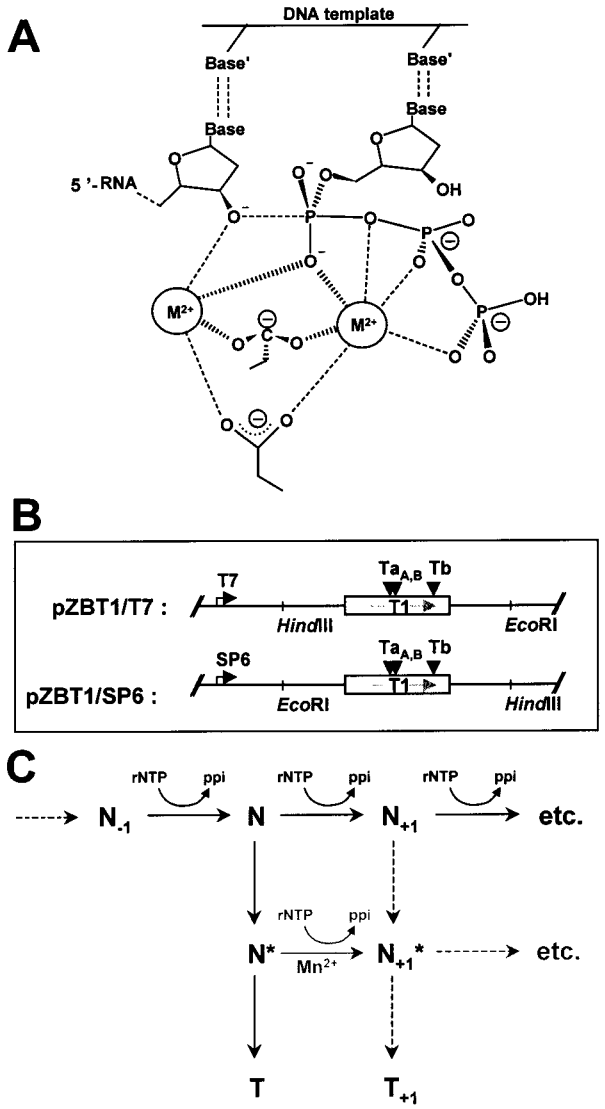

FIGURE 1: Transcript elongation by RNA polymerases. (A) The universal two-metal ion mechanism utilized by RNAPs to catalyze nucleotide incorporation (adapted from ref *4*). The position of two RNAP carboxylate groups and their interaction with metal ions are presented in a generic form and may vary from one enzyme to another. The M^{2+} ion on the left side of the figure is predicted to favor nucleophilic attack of the 3′-OH moiety by lowering its pK_a and to participate in stabilization of the developing negative charge of the pentacovalent transition state. Likewise, the second M^{2+} ion interacts with apical and equatorial oxygens of the pentacovalent phosphate and facilitates departure of the pyrophosphate moiety. (B) Schematic of the DNA templates used in this work. The positions of class I ($Ta_{A,B}$) and class II (Tb) termination sites are denoted with black triangles. (C) Minimal scheme for termination of transcription at the N position. The transcription complex (N) may be converted into a noncompetent state (N*) or continue elongation (N_{+1} state). Competition between both pathways determines the termination efficiency at the N position (*40*). We propose that Mn^{2+} ions activate the N* intermediate and favor escape from the N termination site through the pathway shown in gray. Dashed arrows represent pathways that could also contribute to the establishment of a new distribution of termination products (see the text).

disruption of the interaction between the transcript and its RNA binding site on RNAP due to the formation of the hairpin (*13*, *16*, *18*). The hairpin stem could also invade the upstream edge of the U-rich RNA−DNA hybrid within the transcription bubble, leading to bubble collapse and dissociation of the ternary complex (*15*−*17*). Alternatively, dissociation of the complex may result from pulling the RNA out of the RNAP upon hairpin formation (*19*). In contrast to class I terminators, class II signals do not rely on secondary structures in the transcript but require the 5′-ATCTGTT sequence in the nontemplate DNA strand that often precedes or overlaps with a second T-rich stretch (*10*, *11*, *20*−*22*). Despite these and other differences (*10*, *11*, *20*, *21*), class II signals also mediate formation of a poorly active conformation of the transcription complex prior to RNA release (*23*). Thus, the impediment of catalysis is key to both classes of signals, probably because it ensures for the various components of each terminator the appropriate time frame and topological register within the ternary transcription complex (*1*, *11*, *16*, *23*). However, how impediment of catalysis is achieved within the intermediate complexes has not yet been fully elucidated. By finding and characterizing conditions that restore RNAP catalysis at intrinsic termination sites, we now show that these signals can promote limited perturbations of the catalytic coordination network and can therefore inactivate transcript elongation without relying necessarily on the extrusion of reactants from the RNAP active site.

MATERIALS AND METHODS

Materials. Wild-type and mutant T7 RNAPs were prepared as described previously (*24*, *25*). The SP6 RNAP was purchased from Promega. Most chemicals were from Sigma-Aldrich, while modification enzymes were obtained from New England Biolabs. The rNTP and rNTPαS derivatives as well as radioactive materials were purchased from Amersham.

The pZBT1/T7 and pZBT1/SP6 plasmids (2642 base pairs each) were obtained by subcloning double-stranded synthetic oligonucleotides containing the T1 terminator sequence of the rrnB gene of *Escherichia coli*, in either the sense or antisense orientation (Figure 1B), within the *Sma*I site of plasmid pSP73 (Promega) that is located between convergent T7 and SP6 promoters. For the transcription assays, plasmids pZBT1/T7 and pZBT1/SP6 were linearized with *Eco*RI and *Hin*dIII, respectively. Both plasmids yield runoff transcripts that have a length of 262 nucleotides and termination products that have lengths in the range of 90−130 nucleotides.

Transcription Experiments. For multirun transcriptions, mixtures contained 0.3 pmol of the appropriate linearized plasmid, 6 mM $MgCl_2$, 10 mM NaCl, 20 mM HEPES (pH 7.5), 5 mM DTT, 0.01% Triton X-100, 2 mM spermidine, rNTPs (0.5 mM each), 3 pmol of [α-^{32}P]rUTP, the desired amount of $MnCl_2$, and 1 pmol of T7 (or SP6) RNAP in a final reaction volume of 20 μL. The mixtures were incubated for 30 min at 37 °C. Then, transcription products were resolved by 8 or 10% denaturing polyacrylamide gel electrophoresis. Gel bands were detected and quantified by Phosphorimager (ImageQuant) scanning. Termination efficiencies were derived from normalized band intensities of termination products and read-through transcripts, as described previously (*21*). In the time-monitored experiments, aliquots were removed at various times from the transcription mixture, the reactions quenched by addition of an equal volume of denaturing loading buffer (95% formamide and 5 mM EDTA), and the aliquots chilled on ice before being loaded on the gel.

For experiments with heparin, the buffer components, DNA template (0.3 pmol), and 0.5 mM rATP, rCTP, and rGTP as well as T7 RNAP (0.1 pmol) were mixed together and incubated 5 min at 37 °C. Then, heparin (0−5 mg/mL) was added, followed 10 s later by a mixture of rUTP (0.5 mM), [α-^{32}P]rUTP (3 pmol), and $MnCl_2$ (1 mM). Transcription mixtures were incubated for 5 min at 37 °C before being loaded on a 10% denaturing polyacrylamide gel. Alternatively, the elongation complexes were first radiolabeled by addition of [α-^{32}P]rATP (3 pmol) to the initial transcription mixture devoid of rATP and then chased for 30 s or 1 min at 37 °C with a mixture of 0.5 mM rUTP, 2 mM rATP, and $MnCl_2$ in the presence (or absence) of 5 mg/mL heparin. Analysis of transcripts was carried out as described above.

Sequencing of Transcript 3′-Ends. Each of four independent pools of transcripts containing phosphorothioate modifications at random positions was obtained by addition of a single NTPαS to a multirun transcription mixture containing 1 mM $MnCl_2$ (see above). The NTP/NTPαS ratios were adjusted according to published protocols (*26*, *27*) to obtain approximately two to three NTPαS incorporations per transcript. After incubation for 1 h at 37 °C, the transcription mixture was applied to a spin-down G50-desalting column (Sigma). The eluate was extracted with phenol and precipitated with ethanol. The transcripts in the pellet were labeled with [^{32}P]pCp and T4 RNA ligase, as described previously (*11*). The individual transcripts species within the Ta and Tb clusters were then purified by 10% denaturing polyacrylamide gel electrophoresis and the phosphorothioate linkages cleaved with iodine, as described previously (*26*). Cleavage products were resolved on a 24% denaturing polyacrylamide gel.

RESULTS

The study of intrinsic mechanisms of transcription regulation with the T7 bacteriophage RNAP presents many advantages. Both single-run and multirun transcription experiments are readily carried out in simple media that do not contain initiation or elongation protein cofactors. Experiments, in particular those based on functional mutagenesis, are also facilitated by the monomolecular nature of T7 RNAP as well as by the published structures of the enzyme in various contexts (*28*−*30*). Moreover, despite the absence of sequence homology between bacteriophage and multisubunit RNAPs, a large body of evidence infers common mechanistic features for regulation of transcript elongation (for a detailed discussion, see ref *18*).

The bacterial T1 intrinsic terminator promotes termination of transcription by the T7 and SP6 RNAPs (*22*, *31*). Interestingly, the T1 sequence contains both class I and class II termination signals for the bacteriophage RNAPs (*11*). Thus, with the T1 sequence, two mechanistically distinct intrinsic termination signals can be probed simultaneously (the class I and class II sites within T1 were arbitrarily named the Ta and Tb sites, respectively; Figure 1B). To gain insight into the mechanisms utilized by these signals to inactivate transcript elongation (a prerequisite event of the termination pathway), we have used the classical strategy of "system perturbation" and searched for factors that can affect termination at T1 during transcription with bacteriophage RNAPs. We have focused our attention on factors that can target the catalytic arrangement of reactants as it is the central stage of the elongation process. Hence, single-point mutations of the active site of T7 RNAP, metal ions with coordination features different from those of Mg^{2+}, and cosolvents that can perturb the RNAP interior were assayed. During the course of this study, we have observed an unexpected concentration-dependent effect of Mn^{2+} ions on T1 termination. The extensive characterization of this effect together with its mechanistic implications is presented below.

Effect of Mn^{2+} Ions on Termination of Transcription at the Ta and Tb Sites of the T1 Terminator. Transcriptions with T7 RNAP and a DNA template containing the T1 terminator sequence (Figure 1B) were performed in the presence of various salts and neutral solutes. Remarkably, addition of Mn^{2+} to the transcription mixture yields new and longer transcripts at the T1 hairpin-dependent termination site (Ta), while termination at the downstream site (Tb) is not significantly affected (Figure 2A). Moreover, the new transcripts are formed at the expense of the original Ta termination products (Figure 2A). None of the other salts and solutes that were tested {including K^+, Zn^{2+}, Ca^{2+}, Cd^{2+}, Co^{2+}, Fe^{2+}, $[Co(NH_3)_6]^{3+}$, Ac^-, HPO_4^{2-}, SO_4^{2-}, Glu^-, spermine, sucrose, methanol, and glycerol} induced such changes (data not shown). Similarly, the new distribution of Ta transcripts triggered by Mn^{2+} ions is independent of the nature of buffer (HEPES, MOPS, or Tris-HCl), the concentration of DTT (1−10 mM), the amount of RNAP (0.1−10 pmol), or the topological state (linear or supercoiled) of the DNA template (data not shown). On the other hand, the differential effect of Mn^{2+} on the two termination signals (Ta and Tb) suggests that the evolution of Ta products into longer transcripts does not result from nonspecific initiation or slippage before the enzyme reaches T1 (see also the mapping of RNA 3′-ends, below). Moreover, incubation of purified Ta transcripts (A or B species in Figure 2) with T7 RNAP, rNTPs, and $MnCl_2$ in transcription buffer does not lead to the addition of extra nucleotides to the transcripts (Figure 3A), suggesting that the effect of Mn^{2+} takes place within ternary transcription complexes. Thus, it appears from these data that Mn^{2+} cations alter some specific features of the Ta signal.

Mn^{2+}-Dependent Transcripts Are Products of a Termination Event. To analyze further the new transcripts formed by T7 RNAP in the presence of Mn^{2+} ions, multirun transcription experiments were monitored as a function of time. As shown in Figure 3B, an accumulation of the longer Ta transcripts (B and C species) at the expense of the shortest species (A) is observed at the earliest time points until a constant distribution of Ta products is obtained. This short delay (15−20 s) is a rough estimate of the time required by Mn^{2+} ions to trigger the formation of the longer Ta transcripts. On the other hand, the overall termination efficiency at Ta does not vary with time, indicating that the longer Mn^{2+}-dependent products do not result from transcription complexes that are paused or arrested downstream from the Ta site. Indeed, in the case of a pausing event with a half-life longer than a few seconds (the time frame of the experiment), a decrease in the proportion of the Ta products as a function of time should have been observed (*21*). On the other hand, at a RNAP/template ratio of >1 (our standard conditions; see Materials and Methods), transcription complexes arrested at Ta should have constituted roadblocks for

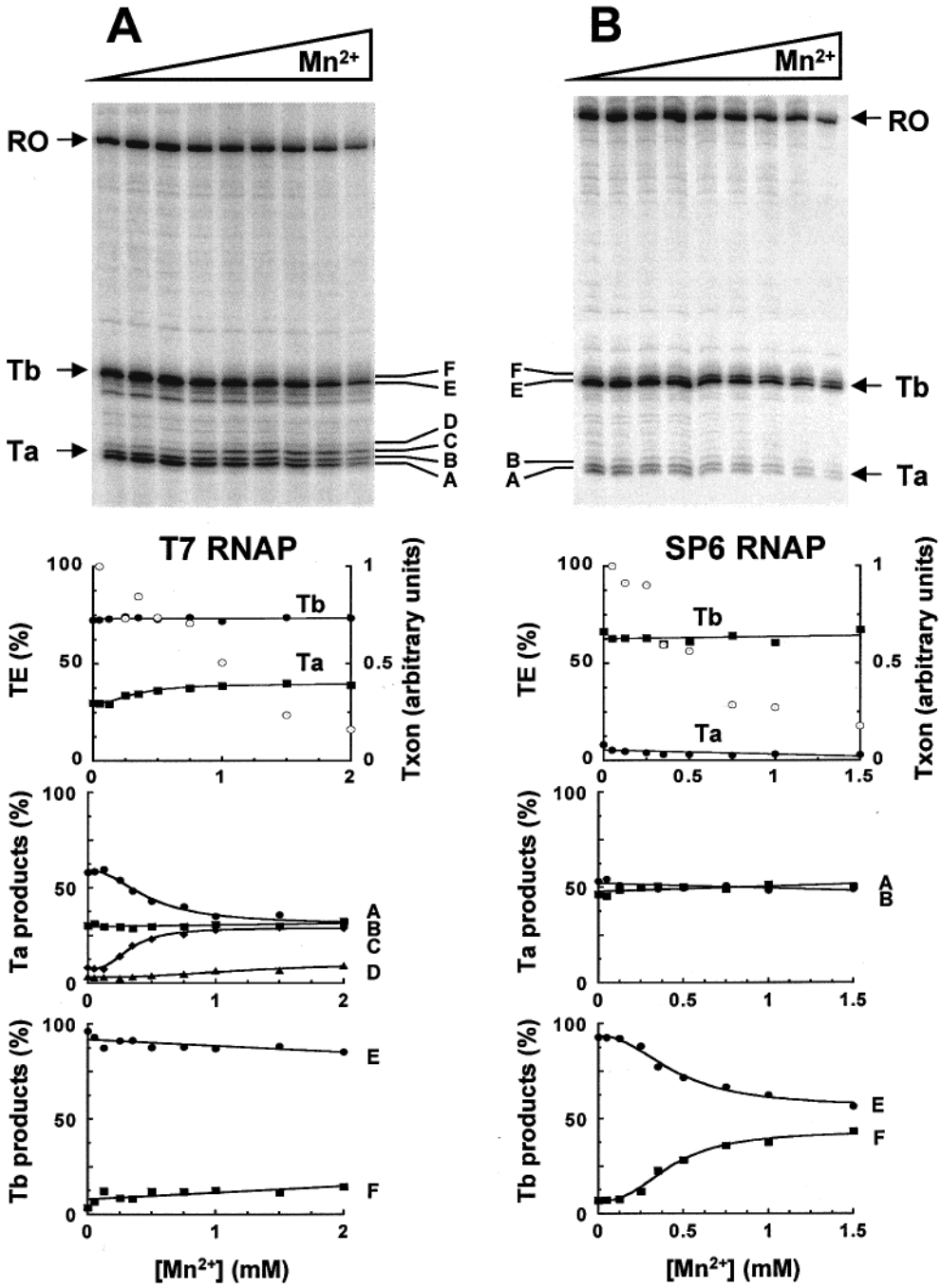

FIGURE 2: Effect of Mn^{2+} ions on termination of transcription at the Ta and Tb sites of the T1 terminator with (A) T7 RNAP and (B) SP6 RNAP. Termination (A−F) and runoff (RO) products were resolved on 10% denaturing polyacrylamide gels (top). For each gel, the lanes correspond to transcription mixtures containing 0, 0.05, 0.125, 0.25, 0.35, 0.5, 0.75, 1, and 1.5 mM $MnCl_2$. For each termination site, the overall termination efficiency (TE) and the product percentages are plotted as a function of Mn^{2+} concentration below the gels. Standardized transcription efficiencies (Txon) are also shown (○). Solid lines are fits of the data to cooperative binding isotherms (*44*) from which Mn^{2+} association parameters were deduced (Table 1). When variations were absent or equivocal in the tested range of Mn^{2+} concentrations, data were arbitrarily fitted to a linear equation. Alteration of transcription termination with T7 RNAP occurs at the Ta site upon binding of 2.3 ± 0.3 Mn^{2+} ions with an apparent K_d of 0.4 ± 0.1 mM (Table 1). Likewise, modification of the product ratio at Tb during transcriptions with SP6 RNAP depends on binding of 2.1 ± 0.6 Mn^{2+} ions with an apparent K_d of 0.45 ± 0.06 mM.

upstream RNAPs leading to an accumulation of shorter transcripts. The data are thus consistent with the release of the Mn^{2+}-dependent Ta products from the ternary transcription complexes which was also confirmed with a nitrocellulose filter binding assay (Figure 3C). Therefore, Mn^{2+} does not fully restore the processivity of the transcription complexes at Ta but triggers the extension of the RNA 3′-ends by a few more nucleotides prior to the dissociation of the complexes.

Mn^{2+}-Directed Incorporation of Additional Nucleotides Is Faithful to the Template Message. It is well-known that Mn^{2+} ions can favor misincorporation of nucleotides within transcripts or promote nontemplated incorporation of nucleotides (*32*, *33*). Similarly, Mn^{2+}, but not Mg^{2+}, can activate phosphorolysis with *E. coli* RNAP, a reaction that is mechanistically related to NTP incorporation and that depends on the presence of an incorrect nucleotide at the RNA 3′-end (*34*). It was thus important to identify the

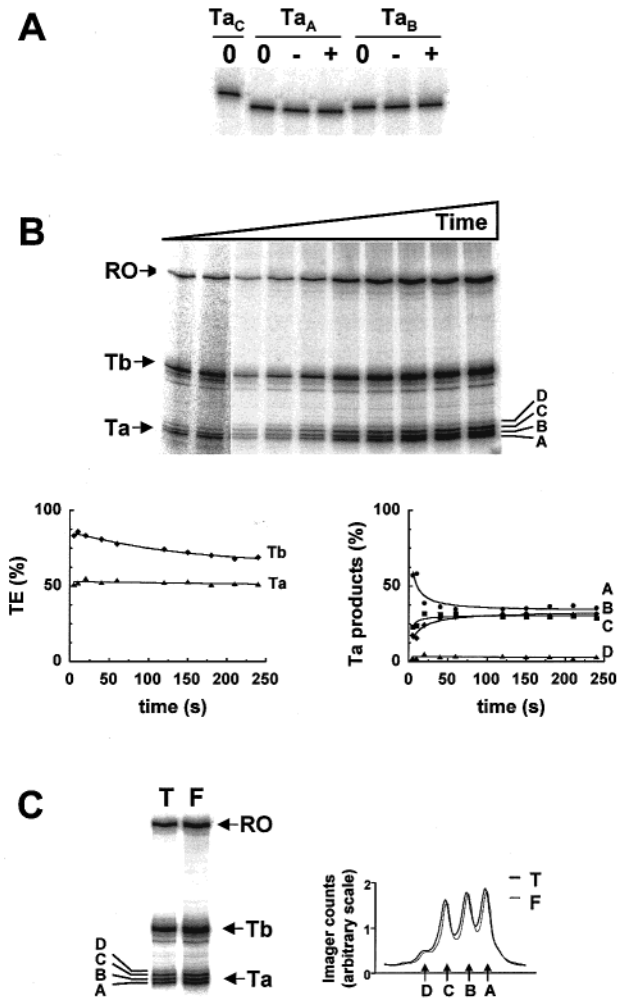

FIGURE 3: Release of Mn^{2+}-dependent Ta transcripts from T7 RNAP transcription complexes. (A) The Mn^{2+}-dependent transcripts are not formed within binary complexes of T7 RNAP and Ta transcripts. Ta transcripts A−C (Figure 2) were prepared in a standard transcription reaction (see Materials and Methods) and purified by 10% denaturing polyacrylamide gel electrophoresis. Individual transcript species (lanes 0), at concentrations of 5−20 nM, were then incubated for 15 min at 37 °C in transcription buffer with T7 RNAP (50 nM) and rNTPs (0.5 mM) with (+) or without (−) 1 mM $MnCl_2$ before being loaded onto a 10% denaturing polyacrylamide gel. (B) Kinetics of multirun transcription of the pZB-T1/T7 template with T7 RNAP in the presence of 1 mM $MnCl_2$. A representative 10% denaturing polyacrylamide gel is shown (gel lanes correspond to aliquots withdrawn from the reaction mixture after incubation for 5, 10, 20, 40, 60, 120, 150, 180, 210, and 240 s at 37 °C). Note that the left part of the gel (the two earliest time points) has been overexposed. Below the gel, the termination efficiencies at the Ta and Tb sites and the percentages of the Ta transcripts are plotted as a function of time. (C) Transcript release evaluated by a nitrocellulose filter binding assay. The experiment and controls were performed as described previously (*45*) with one minor modification, the washing solutions containing 10 mM NaCl. On the gel, the transcripts before loading of the transcription mixture on the nitrocellulose filter (lane T) and those that were not retained on the filter with T7 RNAP (filter eluate; lane F) are compared (gel scans of the Ta region are also presented for both lanes).

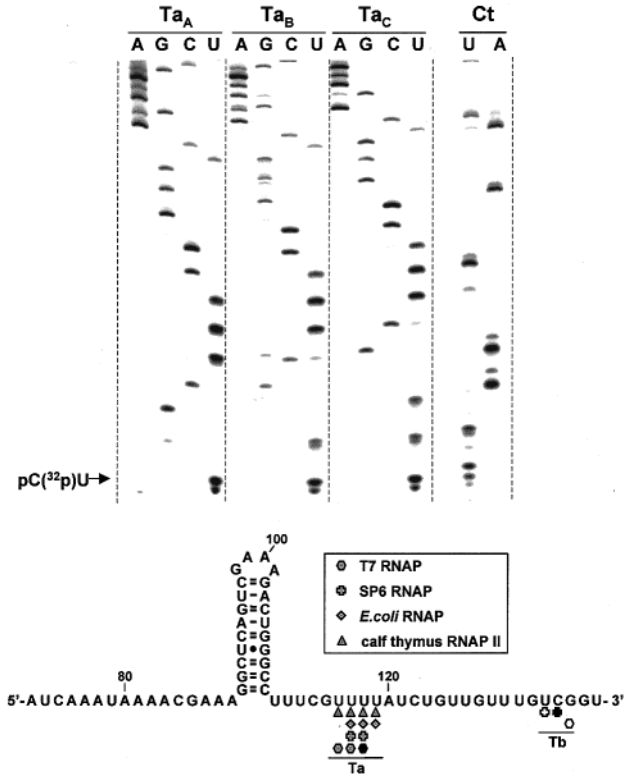

FIGURE 4: Identification of the 3′-ends of the T1 termination products by phosphorothioate sequencing. The normal ($Ta_{A,B}$) and Mn^{2+}-dependent (Ta_C) transcripts randomly modified with the NTPαS shown above the gel lanes were 3′-end-labeled with [^{32}P]-pCp and purified as described previously (*11*). Phosphorothioate linkages were then cleaved with iodine (*26*), and the reaction mixtures were loaded on a 24% denaturing polyacrylamide gel. Note that iodine cleavage of a given phosphorothioate linkage yields a doublet which is resolved only for very short fragments (*26*) and that a slight cross-contamination is observed in the A sequencing lanes for the Ta_A and Ta_B products. The Ct lanes refer to the sequencing of a control RNA having the 3′-end sequence 5′-UCGAAUU-3′. The 3′-ends of the Tb transcripts formed during transcription with SP6 RNAP were identified similarly (not shown). The sequence of the T1 terminator is presented below the gel (numbers refer to the nucleotide positions with respect to the +1 transcription start site of T7 RNAP). The RNA 3′-termini produced by T7, SP6, *E. coli* RNAPs, and calf thymus RNAP II (refs *11*, *22*, *31*, *46*, and *47* and this work) are denoted on the putative secondary structure of the nascent transcript (key is inset). Gray and white symbols correspond to RNA hairpin (Ta)- or DNA template (Tb)-mediated termination events, respectively (*11*). The last 3′-nucleotide of each Mn^{2+}-dependent termination species is identified with a black symbol.

nucleotides incorporated at the 3′-end of the Ta transcripts in the presence of Mn^{2+} ions. This task was accomplished by phosphorothioate sequencing (*26*). Transcription mixtures containing 1 mM $MnCl_2$ were doped with rNTPαS analogues which are substrates of T7 RNAP (*26*). The presence of rNTPαS in the reaction mixture did not interfere with the transcription pattern (data not shown). After isolation and 3′-end labeling of the individual Ta transcript species, the phosphorothioate linkages were cleaved with iodine and the resulting products were resolved by gel electrophoresis (see Materials and Methods). The results, which are presented in Figure 4, demonstrate that the additional nucleotide incorporations triggered by Mn^{2+} ions at the Ta site remain essentially faithful to the template message (see also the results with SP6 RNAP, below). However, it is not possible to determine unambiguously from these data whether products C derive from one or both upstream Ta transcripts (see Figure 1C and below).

Effect of Mn^{2+} Ions on Termination of Transcription with Active Site Mutants of T7 RNAP. The evolution of the Ta

Table 1: Mn^{2+}-Dependent Evolution of Ta Products into Longer Transcripts during Transcriptions with Wild-Type and Active Site Mutants of T7 RNAP[a]

	WT	Y639F[b]	D537E[c]	D812E
n^a	2.3 ± 0.3	2.0 ± 0.4	2.5 ± 0.4	2.0 ± 0.5
$K_d{}^a$ (μM)	382 ± 64	414 ± 52	1563 ± 317	1087 ± 125

[a] The percentages of Ta products as a function of Mn^{2+} concentration were determined from two to three independent experiments. Data were best fitted to equations describing cooperative binding of n Mn^{2+} ions to T7 RNAP (*44*; as shown in Figures 2 and 5). This differs from a previous work in which a model for n equivalent noninteracting binding sites had been used to describe Mn^{2+} binding to free RNAP (*35*). The origin of this discrepancy is unknown but may arise from experimental differences (elongation complex vs free RNAP, for instance). Moreover, competitive binding by Mg^{2+} ions has been neglected because the K_d values for Mg^{2+} are not known precisely and because Mg^{2+} is a very poor competitor to Mn^{2+} binding (approximately half of wild-type T7 RNAP binding sites are occupied by Mn^{2+} ions at a Mg^{2+}/Mn^{2+} ratio of 25; *35*). Simulation of competitive binding with a $K_d(Mg^{2+})$ of 2 mM estimated for the wild-type enzyme (*35*) yields a $K_d(Mn^{2+})$ of 161 ± 28 μM (not shown), in reasonable agreement with the apparent K_d value shown in the table. [b] In contrast to the D537 and D812 residues, Y639 does not participate in binding to metal ions (*35*). [c] For optimal activity of the D537E mutant, the Mg^{2+} concentration in the transcription mixture was increased to 10 mM.

products into longer transcripts is not linear within the range of the Mn^{2+} concentrations that was tested (Figure 2A). In effect, the alteration of the distribution of Ta products depends on cooperative binding of two Mn^{2+} ions with an apparent K_d of 0.4 mM (Figure 2A and Table 1) which corresponds remarkably to the parameters for binding of Mn^{2+} to the active site of T7 RNAP (*35*). As no other manganese ions bind specifically to the T7 enzyme in this concentration range (*35*), it is likely that Mn^{2+} ions affect Ta termination by substituting for the two catalytic Mg^{2+} ions within the RNAP active site (Figure 1). To strengthen this conjecture, additional transcription experiments were performed with T7 RNAP mutants. The mutation of amino acid Y639, a residue implicated in the recognition of the 2′-OH moiety of the incoming rNTP within the active site (*36*, *37*), does not perturb significantly the Mn^{2+}-dependent change in the distribution of Ta products (Figure 5 and Table 1). In contrast, the evolution of Ta products into longer transcripts occurs at much higher Mn^{2+} concentrations upon mutation of either of two amino acids (Asp537 and Asp812; see Figure 5 and Table 1) that participate in metal ion binding within the RNAP active site (*35*). Thus, there is a direct relationship between the strength of binding of Mn^{2+} ions to the active site and their effect on Ta termination which supports an action of the metal ions directly on (or from) the RNAP active center.

The mutation of amino acids within the RNAP active site also alters differently the response of the transcription complexes to termination signals. With the Y639F mutant, termination efficiencies at the Ta and Tb sites are similar to the ones observed with the wild-type enzyme and do not vary when Mn^{2+} is added to the transcription mixture (Figure 5). This suggests that active site contacts to the 2′-OH moiety of the incoming rNTP are not involved in the termination mechanisms. In contrast, the D537E and D812E mutants are extremely sensitive to the termination signals, and in the absence of Mn^{2+} ions, they almost completely fall off the DNA template at the first release site (Ta site; Figure 5 and data not shown). Thus, the lengthening of either side chain by one methylene group (Asp → Glu mutations), which alters the metal ion coordination within the active site and reduces the enzyme catalytic activity (*35*), renders the T7 RNAP termination-prone. However, the D537E and D812E enzymes can partially read through termination sites when Mn^{2+} ions are present in the reaction mixture, the amount of read-through transcripts increasing in the $MnCl_2$ concentration range of 0.2−3 mM (Figure 5 and data not shown). Thus, in the case of the D537E and D812E mutants, Mn^{2+} ions have a dual effect: triggering the evolution of Ta termination products into longer transcripts, as with the wild-type enzyme, and partially shielding the transcription complexes from termination events.

Mn^{2+} Ions Trigger Phosphoryl Transfer Reactions within a Heparin-Sensitive Transcription Complex. Taken together, the data suggest that two Mn^{2+} ions within the active site can potentiate the catalytic features of a transcription complex located at a termination site (thus promoting additional incorporations of nucleotides within the transcript). This can lead to the escape of the transcription complex from the termination signal (as in the case of the D537E and D812E mutants) or to the limited extension of the 3′-ends of transcripts prior to the dissociation of the ternary complexes. In the latter case, Mn^{2+} ions cannot offset the components of the termination signal that are responsible for transcript release, suggesting that the transcription complex is already engaged in the termination pathway (N* intermediate in Figure 1C). To support this view, the effect of Mn^{2+} on Ta termination was assessed as a function of the stability of the transcription complex, one feature that could depend on the state of the ternary complex (N or N*) (*16*, *21*, *38*). In a modified experimental setup, the transcription ability of T7 RNAPs that were not engaged in stable transcription complexes was challenged by the addition of heparin to the reaction mixture (see Materials and Methods). As shown in Figure 6A, the amount of Mn^{2+}-dependent Ta products decreases as a function of heparin concentration and reverts to background levels when conditions of single-run transcription are approached (that is when the concentration of heparin is sufficient to prevent RNAP recycling and transcription initiation). To determine whether the disappearance of the Mn^{2+}-dependent Ta products is related to the modification of the kinetic regimen induced by heparin (from multirun to single-run transcription conditions), experiments in which only the first run of transcription is monitored (see Materials and Methods) were also performed. Under these conditions, the formation of the longer Mn^{2+}-dependent Ta products is still observed, and it is also inhibited by the presence of heparin (Figure 6B). These results show that the Mn^{2+}-dependent evolution of Ta transcripts is not coupled to multirun events and that the effect of heparin takes place during the elongation phase of transcription. Yet, the additional nucleotide incorporations triggered by Mn^{2+} ions at the Ta site occur within a transcription complex that is sufficiently unstable to allow heparin to competitively displace RNAP from it. Similar results were obtained with KCl as the challenging agent (data not shown), suggesting that ionic interactions predominate within the unstable transcription complex. In both respects (instability and predominant ionic interactions), this complex differs greatly from stable elongating transcription complexes (*16*, *21*, *38*)

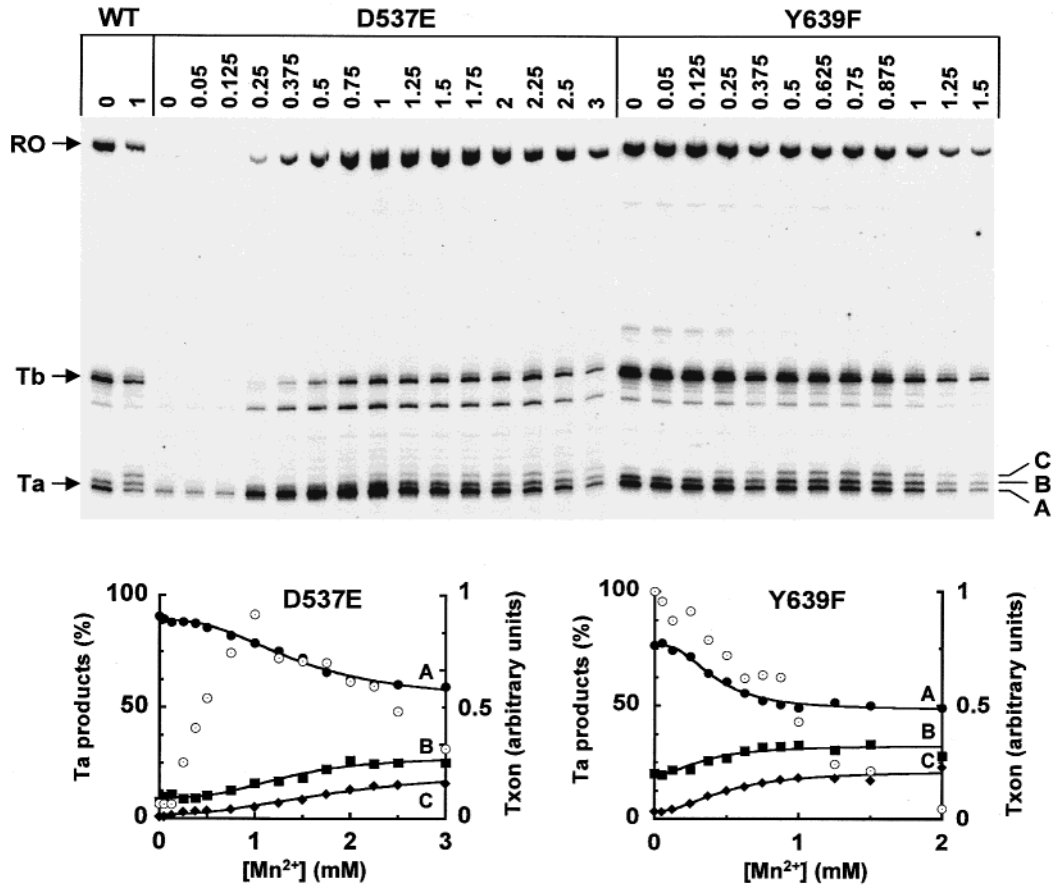

FIGURE 5: Effect of Mn^{2+} ions on termination of transcription at the Ta and Tb sites with active site mutants of T7 RNAP. The concentrations of $MnCl_2$ (in mM) in the transcription mixtures are indicated above the gel lanes. For each mutant, the percentages of Ta products are plotted as a function of Mn^{2+} concentration below the gels. Transcription efficiencies relative to the reaction without manganese are also shown (○). The legend and the fits to the experimental data are as in Figure 2. Note that with the D537E and D812E mutants, the minor band between the Ta and Tb sites becomes stronger, suggesting that it may correspond to a low-efficiency termination event.

and corresponds best to the N* intermediate in Figure 1C. Thus, Mn^{2+} ions specifically promote the addition of nucleotides to the transcript 3′-end within a transcription complex that has experienced extensive modifications and that has presumably already entered the termination pathway.

Effect of Mn^{2+} Ions on Transcription of the T1 Template with the SP6 RNAP. Interestingly, Mn^{2+} alters T1 termination of transcription with SP6 RNAP at the downstream Tb site rather than at Ta (Figure 2B). It is the Tb products that evolve into longer transcripts as a function of Mn^{2+} concentration, whereas Ta termination products remain unaffected. It has been deduced from phosphorothioate sequencing that the new Tb transcripts contain one additional C residue at their 3′-tip (not shown). This result unambiguously rules out transcript slippage as an alternative mechanism, while it supports template-dependent elongation of the Tb transcript by one nucleotide (see the sequence of Tb in Figure 4). Moreover, the evolution of Tb products into longer transcripts depends on the cooperative binding of two Mn^{2+} ions with an apparent K_d of ~0.4 mM (Figure 2B). Together with the results of the experiments performed with T7 RNAP, these results argue against an effect on termination originating from binding of Mn^{2+} ions to a given RNA or DNA motif because the Ta and Tb signals rely on distinct RNA and DNA elements (*11*, *21*). On the other hand, the data also show that the effect of Mn^{2+} ions on intrinsic termination is context-dependent as it can vary as a function of the RNAP and the termination signal.

DISCUSSION

In this paper, we show that two Mn^{2+} ions within the active site of bacteriophage RNAPs can promote the template-directed addition of one or two nucleotides to the 3′-ends of the transcripts when the transcription complexes are located at intrinsic termination sites. This unusual transcript elongation occurs within transcription complexes that are unstable (sensitive to heparin and high-salt conditions). Moreover, Mn^{2+} ions can also help termination-prone active site mutants of T7 RNAP to overcome transcript release and to read through termination sites.

There are different possible ways by which the Mn^{2+} ions can induce the evolution of Ta termination products into longer transcripts prior to the dissociation of the ternary complexes. (i) They could increase the T7 RNAP elongation rate and thus favor escape of the ternary complex from the normal termination sites (*39*, *40*). However, this mechanism appears to be unlikely because an increase in transcription efficiency and a reduction in the extent of transcription termination should also be observed (*39*), which is not the case with the Y639F and wild-type enzymes (Figures 2A and 5). On the other hand, an increase in the elongation rate could be a factor by which Mn^{2+} ions cause the D537E and

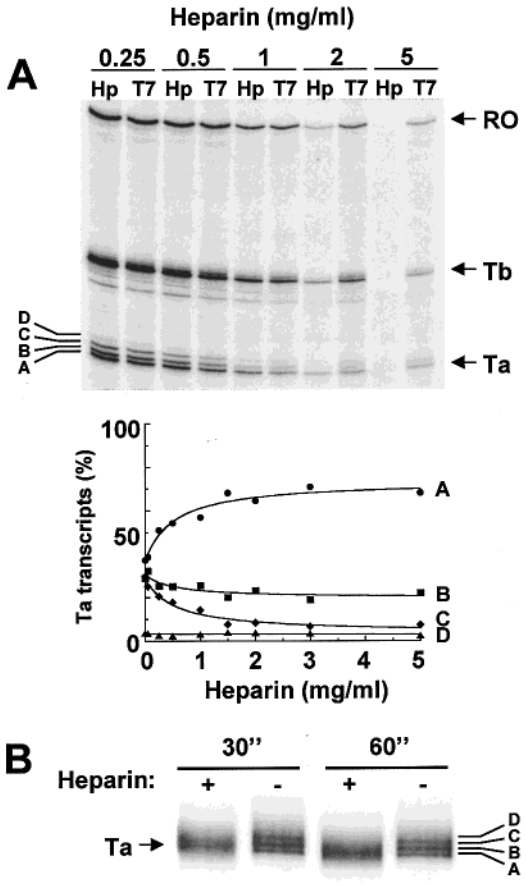

FIGURE 6: Effect of heparin on the distribution of the transcript species formed at the Ta site in the presence of Mn^{2+} ions. (A) Elongating transcription complexes were preformed and stalled at position 12 by privation of rUTP (*21*, *38*). Then, heparin (0−5 mg/mL), rUTP, [α-^{32}P]rUTP, and $MnCl_2$ (1 mM) were added (see Materials and Methods). Reaction mixtures were incubated for 5 min at 37 °C before being loaded on a 10% denaturing polyacrylamide gel (lanes T7). In control experiments (lanes Hp), heparin was added prior to T7 RNAP. Gel bands are labeled as in Figure 2. A heparin concentration of 5 mg/mL was necessary to completely inhibit initiation of transcription by free RNAP molecules and reach conditions of single-run transcriptions. In contrast, ∼2−3 mg/mL heparin was sufficient to obtain a distribution of Ta termination products similar to the one observed in the absence of Mn^{2+} ions. (Data points are mean values from three independent experiments with a standard deviation of ≤25%. However, because of the very weak signals at high heparin concentrations, potential variations in the amounts of species D are below the detection limit and could not be determined accurately.) (B) In a control experiment, the elongation complexes stalled at position 12 were labeled by addition of [α-^{32}P]rATP to the initial transcription mixture devoid of unlabeled rATP and then chased for 30 or 60 s at 37 °C with rUTP (0.5 mM), rATP (2 mM), and $MnCl_2$ (1 mM) in the presence (+) or absence (−) of 5 mg/mL heparin. Under these conditions, the incorporation of [α-^{32}P]rATP during the chase is negligible (<10%), and labeled transcripts correspond essentially to the first run of transcription (single-run conditions). However, as shown in the enlarged view of the Ta region that is presented in the figure, the limited quality of the data that was consistently observed under these experimental conditions only permits qualitative analysis.

D812E mutants to read through termination sites (see below). (ii) Mn^{2+} ions could increase the stability of the ternary complexes. However, once again, such a mechanism would favor the escape of the complexes from the termination points and a decrease in termination efficiencies for the wild-type and Y639F enzymes. Moreover, the heparin and high-salt experiments (see the Results) suggest that the stability of the intermediate complex (N*) remains very low, even in the presence of Mn^{2+} ions. Additionally, it is difficult to envision how two Mn^{2+} ions within the RNAP active site could affect the stability of the ternary complex, unless some unknown allosteric mechanism is involved. (iii) Mn^{2+} ions could delay the termination event and thus permit further transcript elongation, but the effect of Mn^{2+} ions occurs within a complex that strongly differs from stable elongating complexes (see above), indicating that the termination process has already started. (iv) Mn^{2+} ions could compensate for modifications of the transcription complex induced by the termination signal. This is the most likely explanation because the Mn^{2+} ions act within a ternary complex that is already engaged in the termination pathway (see above).

It is postulated that the signals that regulate transcript elongation induce disruptive conformational changes of the ternary transcription complexes (*6*−*8*, *16*, *17*, *21*, *40*). In the case of the termination signals, these changes are irreversible and lead to the dissociation of the ternary complex (*16*, *21*). However, intrinsic termination events first initiate the conversion of the transcription complex into a transient and catalytically incompetent intermediate that subsequently undergoes dissociation (*9*, *15*−*17*, *23*). The Mn^{2+} ions trigger the addition of nucleotides to the 3′-end of the Ta transcripts within a heparin and salt-sensitive ternary complex. In the absence of Mn^{2+} ions, this complex is unable to promote nucleotide incorporations. Clearly, this unstable and catalytically incompetent complex exhibits features of the intermediate complex that is formed in the termination pathway (*9*, *15*−*17*, *23*). Thus, Mn^{2+} ions in the active site of the unstable intermediate complex can oppose the factors responsible for impediment of catalysis. This could be done by preventing or limiting the reactant extrusion that would result from RNAP sliding along the template or from pulling out of the RNA 3′-end. However, the molecular mechanism underlying this process would remain elusive. Alternatively, the termination signal could bring about a limited alteration of the catalytic arrangement of reactants and metal effectors like the one proposed recently for hairpin-dependent pausing (*17*). Despite a coordination geometry similar to that of Mg^{2+}, Mn^{2+} ions exhibit different and less stringent structural parameters (bond lengths, angular deviations between ligands, preferred binding sites, etc.) during interaction with ligands (*33*, *41*). The relaxation of structural and chemical requirements of Mg^{2+}-dependent phosphoryl transfer enzymes in the presence of Mn^{2+} ions has been attributed to the greater ability of Mn^{2+} to accommodate a wide range of reactive group geometries (*33* and references therein). Accordingly, Mn^{2+} ions could compensate for an altered geometry of the catalytic arrangement of reactants when the RNAP enters the termination pathway, thereby promoting further elongation of the transcript within the unstable intermediate complex. Other effects of Mn^{2+} on the components of the elongation complex (structural modification of RNA or DNA motifs, changes in the K_d values for the incoming rNTP, etc.; see ref *33* and references therein) could also be considered, but none seems to be fully consistent with all the experimental data, even though some may contribute individually to the activation of a distorted catalytic setup (for instance, improved binding of the

incoming rNTP to a distorted RNAP active site may result from preferential chelation of Mn^{2+} by the α- and γ-phosphates of the rNTP; *32*, *33*).

The ability of Mn^{2+} ions to adjust distorted catalytic arrangements is also evident in the case of the D537E and D812E mutants. With these two enzymes, the perturbation of the catalytic coordination network results directly from the active site mutations, and this impairs transcript elongation and favors termination (see the Results). However, Mn^{2+} ions allow the RNAP mutants to transcribe more efficiently and to read through termination signals (Figure 5), thereby compensating for the inadequate geometry of the catalytic arrangement induced by the amino acid mutations. Interestingly, Mn^{2+} also restores catalysis with active site mutants of the polio virus RNA-dependent RNAP that are inactive when only Mg^{2+} ions are present (*42*). In other words, Mn^{2+} ions in an RNAP active site "rescue" distorted catalytic setups; they favor transcript elongation (increase the elongation rate) within the unstable intermediate complexes (N*) formed at termination sites and also during "normal" RNA synthesis with the active site RNAP mutants. During processive elongation with wild-type RNAP, there is no significant kinetic advantage resulting from Mn^{2+} replacement because Mg^{2+} ions accommodate the active site well enough. Moreover, in the case of the RNAP mutants, the Mn^{2+}-induced increase in the elongation rate decreases the termination efficiency because the kinetic competition between elongation and termination is modified. All these data consistently demonstrate that the deviation from an ideal setup of reactants and metal ion effectors does not need to be extensive to impair RNAP catalytic power. This is in agreement with previous work showing that small deviations from optimal orbital steering can strongly decrease enzymatic reaction rates (*43*).

The distribution of termination products at the Ta site depends on the kinetic competition between elongation, inactivation (which is potentially reversible), and complex dissociation at each template position within the termination window (Figure 1C). In the presence of Mn^{2+} ions, a new kinetic pathway is involved which leads to the addition of extra nucleotides to the transcript 3′-ends (Figure 1C). Still, the new distribution of termination products remains dependent on a network of individual kinetic parameters: the ones cited above and the rate of Mn^{2+}-dependent addition of extra nucleotides. To compete efficiently with normal transcript elongation, complex inactivation needs to occur on the same time scale (230 s^{-1} at 37 °C for processive elongation). On the other hand, the Mn^{2+}-dependent addition of extra nucleotides within the intermediate complex appears to be considerably slower (an average elongation rate of <0.3 s^{-1} at 37 °C can be estimated from the time needed to reach a steady-state distribution of Ta transcripts; see Figure 3B). In the case of *E. coli* RNAP, dissociation of the intermediate complex at the *his* termination site is also much slower (300−500 times) than processive elongation or complex inactivation (*40*). This suggests that the evolution of the distribution of Ta transcripts is mostly driven by the kinetic competition between the slow Mn^{2+}-dependent nucleotide incorporation and the dissociation of the unstable ternary complex [reversion to a fully active complex is probably negligible because addition of heparin to the transcription mixture does not significantly increase the termination efficiency at Ta (Figure 6), thereby suggesting that termination efficiency is independent of the fate of the intermediate complex; see also ref *40*]. However, this kinetic competition is not necessarily the same at every template position of the termination window since factors such as the extent of RNAP active site distortion or the complex stability are likely to depend on the location of the intermediate complex along the DNA template. From this perspective, it is even possible that slow Mg^{2+}-driven incorporations of nucleotides take place within unstable intermediate complexes under certain circumstances (dissociation and Mg^{2+}-driven incorporation rates of the same magnitude). Partitioning between nucleotide incorporation and dissociation of the intermediate complex may then contribute to the display of several termination points (usually two) until the unstable complex reaches a template position where dissociation prevails. Further work is in progress to test this proposal more extensively.

It has been proposed that lateral displacements of the ternary transcription complex (such as backtracking) which promote complete extrusion of the RNA 3′-end from the RNAP catalytic center could represent predominant inactivated states at various pause and arrest sites (refs *1* and *9* and references therein). Yet, inhibition of elongation may also be triggered in these cases by a more localized alteration of the enzyme catalytic arrangement earlier on the inactivation pathway. In fact, Landick and co-workers have recently proposed a mechanistic framework in which the different intermediate complexes representative of the various regulatory events (pause, arrest, or termination) arise from the same catalytically deficient precursor (*9*). Thus, one "trick" common to intrinsic blocks to transcription elongation may well be the timely impediment of effective catalysis through limited alteration of the catalytic coordination network within the RNAP active site. This could be due to peculiar structural features of the U-rich hybrid within the transcription bubble (*16*, *39*) that would cause misplacement of the RNA 3′-OH. Alteration of the catalytic arrangement may also result from changes in the tertiary contacts within the transcription complex (changes induced by the formation of the RNA hairpin, for instance) that could be transmitted up to the enzyme active site by an allosteric mechanism (*17*). It has recently been proposed that this task could be carried out by the Flap and Connector domains of *E. coli* RNAP (*17*). Similarly, the specificity loop of T7 RNAP, an analogous structural element, could serve the same function (*18*). The extent of active site deformation would then depend on the RNAP (as "transmitting" and other functional elements may be analogous but not identical in size or shape) and on the specific sterical constraints imposed by a given termination signal (the length of the RNA hairpin, for instance). This, in turn, could explain the context dependence of the Mn^{2+} effect on transcription termination that is observed in this work (for instance, Mn^{2+} does not trigger addition of extra nucleotides to the transcript at Ta with SP6 RNAP and at Tb with T7 RNAP). In effect, even the "relaxed" coordination features of Mn^{2+} ions cannot conceivably accommodate every distorted arrangement of reactants. Finally, because distortions of the catalytic arrangement can have diverse origins and extents, they may also arise from regulatory signals that, otherwise, display significant mechanistic differences (such as class I and class II termination sites).

ACKNOWLEDGMENT

We are grateful to Anna M. Pyle and Konstantin Severinov for critical reading of the manuscript and to Zoubida Boudalaa for her excellent technical assistance. We thank A-Young M. Woody and William T. McAllister for the gift of T7 RNAP mutants as well as the reviewers for insightful comments.

REFERENCES

1. Mooney, R. A., Artsimovitch, I., and Landick, R. (1998) *J. Bacteriol. 180*, 3265−3275.
2. Nudler, E. (1999) *J. Mol. Biol. 288*, 1−12.
3. Steitz, T. A., and Steitz, J. A. (1993) *Proc. Natl. Acad. Sci. U.S.A. 90*, 6498−6502.
4. Steitz, T. A. (1998) *Nature 391*, 231−232.
5. Cramer, P., Bushnell, D. A., and Kornberg, R. D. (2001) *Science 292*, 1863−1876.
6. Erie, D. A., Hajiseyedjavadi, O., Young, M. C., and von Hippel, P. H. (1993) *Science 262*, 867−873.
7. Eichhorn, G. L., Chuknyisky, P. P., Butzow, J. J., Beal, R. B., Garland, C., Janzen, C. P., Clark, P., and Tarien, E. (1994) *Proc. Natl. Acad. Sci. U.S.A. 91*, 7613−7617.
8. Huang, J., Brieba, L., and Sousa, R. (2000) *Biochemistry 39*, 11571−11580.
9. Artsimovitch, I., and Landick, R. (2000) *Proc. Natl. Acad. Sci. U.S.A. 97*, 7090−7095.
10. Macdonald, L. E., Durbin, R. K., Dunn, J. J., and McAllister, W. T. (1994) *J. Mol. Biol. 238*, 145−158.
11. Hartvig, L., and Christiansen, J. (1996) *EMBO J. 15*, 4767−4774.
12. Jeng, S. T., Gardner, J. F., and Gumport, R. I. (1990) *J. Biol. Chem. 265*, 3823−3830.
13. Macdonald, L. E., Zhou, Y., and McAllister, W. T. (1993) *J. Mol. Biol. 232*, 1030−1047.
14. Jeng, S. T., Lay, S. H., and Lai, H. M. (1997) *Can. J. Microbiol. 43*, 1147−1156.
15. Artsimovitch, I., and Landick, R. (1998) *Genes Dev. 12*, 3110−3122.
16. Gusarov, I., and Nudler, E. (1999) *Mol. Cell 3*, 495−504.
17. Toulokhonov, I., Artsimovitch, I., and Landick, R. (2001) *Science 292*, 730−733.
18. Temiakov, D., Mentesana, P. E., Ma, K., Mustaev, A., Borukhov, S., and McAllister, W. T. (2000) *Proc. Natl. Acad. Sci. U.S.A. 97*, 14109−14114.
19. Yarnell, W. S., and Roberts, J. W. (1999) *Science 284*, 611−615.
20. He, B., Kukarin, A., Temiakov, D., Chin-Bow, S. T., Lyakhov, D. L., Rong, M., Durbin, R. K., and McAllister, W. T. (1998) *J. Biol. Chem. 273*, 18802−18811.
21. Lyakhov, D. L., He, B., Zhang, X., Studier, F. W., Dunn, J. J., and McAllister, W. T. (1998) *J. Mol. Biol. 280*, 201−213.
22. Kwon, Y. S., and Kang, C. (1999) *J. Biol. Chem. 274*, 29149−29155.
23. Song, H., and Kang, C. (2001) *Genes Cells 6*, 291−301.
24. Osumi-Davis, P. A., de Aguilera, M. C., Woody, R. W., and Woody, A. Y. (1992) *J. Mol. Biol. 226*, 37−45.
25. He, B., Rong, M., Lyakhov, D., Gartenstein, H., Diaz, G., Castagna, R., McAllister, W. T., and Durbin, R. K. (1997) *Protein Expression Purif. 9*, 142−151.
26. Gish, G., and Eckstein, F. (1988) *Science 240*, 1520−1522.
27. Strobel, S. A., and Shetty, K. (1997) *Proc. Natl. Acad. Sci. U.S.A. 94*, 2903−2908.
28. Sousa, R., Chung, Y. J., Rose, J. P., and Wang, B. C. (1993) *Nature 364*, 593−599.
29. Cheetham, G. M., Jeruzalmi, D., and Steitz, T. A. (1999) *Nature 399*, 80−83.
30. Cheetham, G. M., and Steitz, T. A. (1999) *Science 286*, 2305−2309.
31. Lyakhov, D. L., He, B., Zhang, X., Studier, F. W., Dunn, J. J., and McAllister, W. T. (1997) *J. Mol. Biol. 269*, 28−40.
32. Pelletier, H., Sawaya, M. R., Wolfle, W., Wilson, S. H., and Kraut, J. (1996) *Biochemistry 35*, 12762−12777.
33. Huang, Y., Beaudry, A., McSwiggen, J., and Sousa, R. (1997) *Biochemistry 36*, 13718−13728.
34. Libby, R. T., and Gallant, J. A. (1994) *Mol. Microbiol. 12*, 121−129.
35. Woody, A. Y., Eaton, S. S., Osumi-Davis, P. A., and Woody, R. W. (1996) *Biochemistry 35*, 144−152.
36. Sousa, R., and Padilla, R. (1995) *EMBO J. 14*, 4609−4621.
37. Huang, Y., Eckstein, F., Padilla, R., and Sousa, R. (1997) *Biochemistry 36*, 8231−8242.
38. Mentesana, P. E., Chin-Bow, S. T., Sousa, R., and McAllister, W. T. (2000) *J. Mol. Biol. 302*, 1049−1062.
39. McDowell, J. C., Roberts, J. W., Jin, D. J., and Gross, C. (1994) *Science 266*, 822−825.
40. Yin, H., Artsimovitch, I., Landick, R., and Gelles, J. (1999) *Proc. Natl. Acad. Sci. U.S.A. 96*, 13124−13129.
41. Harding, M. M. (1999) *Acta Crystallogr. D55*, 1432−1443.
42. Jablonski, S. A., and Morrow, C. D. (1995) *J. Virol. 69*, 1532−1539.
43. Mesecar, A. D., Stoddard, B. L., and Koshland, D. E. J. (1997) *Science 277*, 202−206.
44. Cantor, C. R., and Schimmel, P. R. (1980) *Biophysical chemistry: the behavior of biological macromolecules*, Vol. 3, Freeman and Co., San Francisco.
45. Sastry, S. S., and Hearst, J. E. (1991) *J. Mol. Biol. 221*, 1091−110.
46. Dedrick, R. L., Kane, C. M., and Chamberlin, M. J. (1987) *J. Biol. Chem. 262*, 9098−9108.
47. Reynolds, R., Bermudez-Cruz, R. M., and Chamberlin, M. J. (1992) *J. Mol. Biol. 224*, 31−51.

BI011358Q